– Supplementary Information –

The role of the serosa in intestinal anastomotic healing: insights from in-depth histologic analysis of human and murine anastomoses

Original Report

Marie-Christin Weber, MD[1]; Zoé Clees, MD[1]; Annalisa Buck, MSc[1,2]; Adrian Fischer, PhD[3]; Marcella Steffani, MD[1]; Dirk Wilhelm, MD[1]; Marc Martignoni, MD[1], Helmut Friess, MD[1]; Yuval Rinkevich, PhD[3]; Philipp-Alexander Neumann, MD[1,2]

[1]Department of Surgery, Technical University of Munich, TUM School of Medicine and Health, Munich, Germany

[2]Institute for Advanced Study, Technical University of Munich, Munich, Germany

[3]Helmholtz Institute of Regenerative Biology and Medicine at the Helmholtz Center, Munich, Germany

1. Supplementary materials and methods

2.1 Evaluation of anastomotic leakage

Anastomotic leakage was defined as macroscopically visible peritonitis or abscess formation around the anastomosis at sacrifice. Immediately prior to sacrifice, colonoscopy of the descending colon including the anastomosis was performed as described by previously described.[1]

2.2 Adhesion score

Regarding the presence of adhesions around the anastomosis, we scored the adhesion load according to the following parameters:

Supplementary Table 1: *Adhesion score*

Criteria	Score points
Adhesion of uterus, small intestine, omentum, pancreas	
- **no**	0
- **yes**	1 point per organ
Adhesion of other organs (gonadal fat, colon, peritoneum, etc.)	
- **no**	0
- **yes**	1
Removability of adhesions	
- **no adhesions at all**	0
- **all adhesions removable**	1
- **adhesions partially removable**	2
- **adhesions not removable**	3
Adhesions score = sum of all score points	

2. Supplementary results

2.1 Anastomotic leakage in murine model

None of the mice (n = 6 per time-point, total n= 24) showed macroscopically visible peritonitis or abscess formation around the anastomosis at sacrifice. All anastomoses were intact during colonoscopy prior to sacrifice.

2.2 Adhesion score

All anastomoses had some degree of adhesions. The mean adhesion score at POD3 was 4.5±1.05, 4.7±0.82 at POD7, 4.8±0.75 at POD14 and 5.33±0.52 at POD21 (**Supplementary Figure 1A**). The small intestine was the most common organ adherent to the anastomosis, followed adhesions from the omentum, pancreas and uterus (**Supplementary Figure 1B**).

3. Supplementary figures

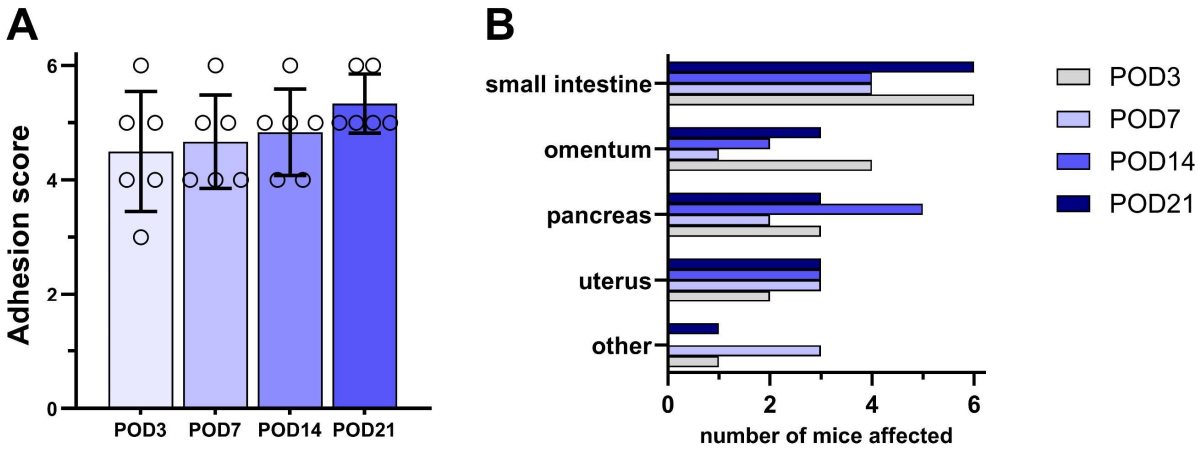

Supplementary Figure 1: Adhesion score and distribution of adhesions according to the adherent organ. (A) Adhesion score according to Supplementary Table 1. Differences between groups were not significant. One-way ANOVA with Tukey's multiple comparison test, data are mean ± SD with dots for individual values. **(B)** Distribution of adhesions according to the adherent organ. X-axis = number of mice affected by adhesion. n = 6 per time-point.

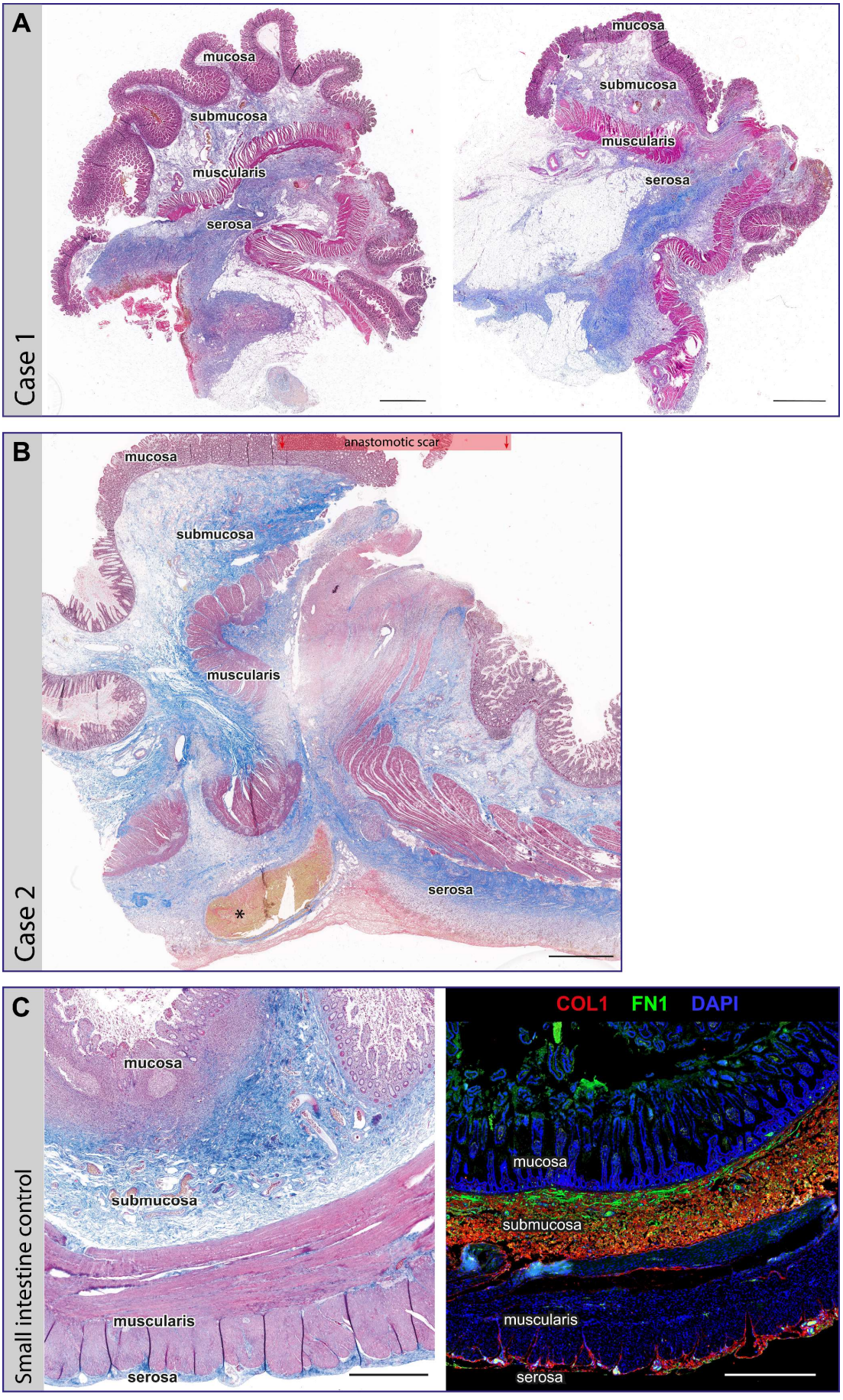

Supplementary Figure 2: Histological evaluation of early postoperative human intestinal anastomosis and control small intestine. (A) Two additional overview scans of Masson's trichrome-stained histologic section of human anastomosis (Case 1) on postoperative day (POD) 7. Scale bar = 2000µm, 400x magnification. **(B)** Overview scan of Masson's trichrome-stained histologic section of human anastomosis (Case 2) on POD9. * = hematoma within serosal scar. Scale bar = 2000µm, 400x magnification. **(C)** Overview scans of Masson's trichrome as well as immunofluorescence [fibronectin (FN1) and type I collagen (COL1)] stained human small intestine control. Scale bar = 1000µm, 400x magnification (left), 100x magnification (right).

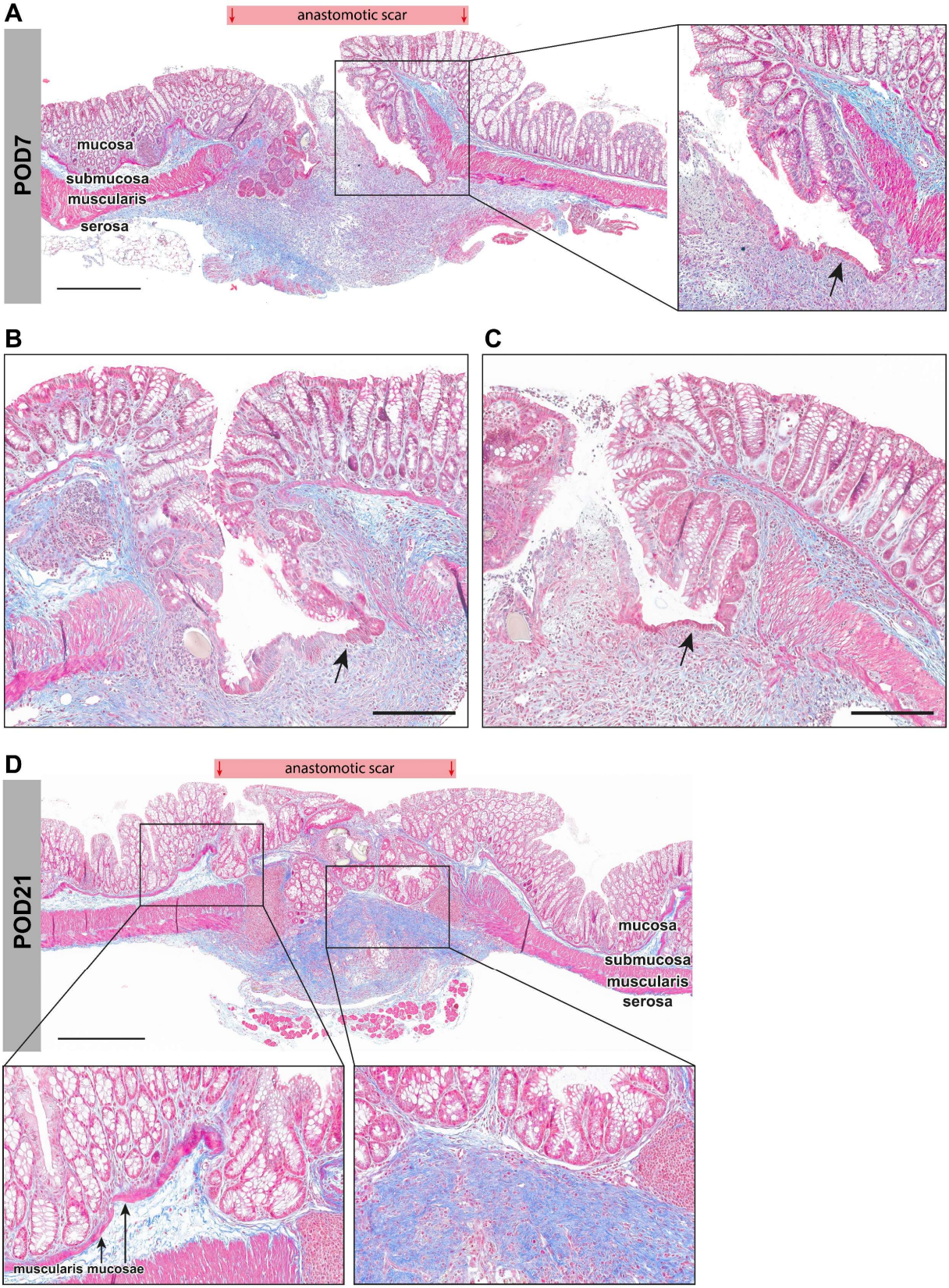

Supplementary Figure 3: Details of histologic evaluation of murine anastomoses. (A) At postoperative day 7 (POD7), the mucosal layer is not completely closed in most cases. It can be observed that a single layer of epithelial cells regenerates on top of the extracellular matrix within the anastomotic scar. Scale bar = 500µm, 400x magnification. (B+C) Two more representative images of epithelial regeneration within the anastomosis. Scale bar = 200µm, 400x magnification. (D) The gap and lack of closure of the muscularis layer is evident in the overview scans. It can also be seen that the lamina muscularis mucosae is absent within the anastomotic scar. Scale bar = 500µm, 400x magnification.

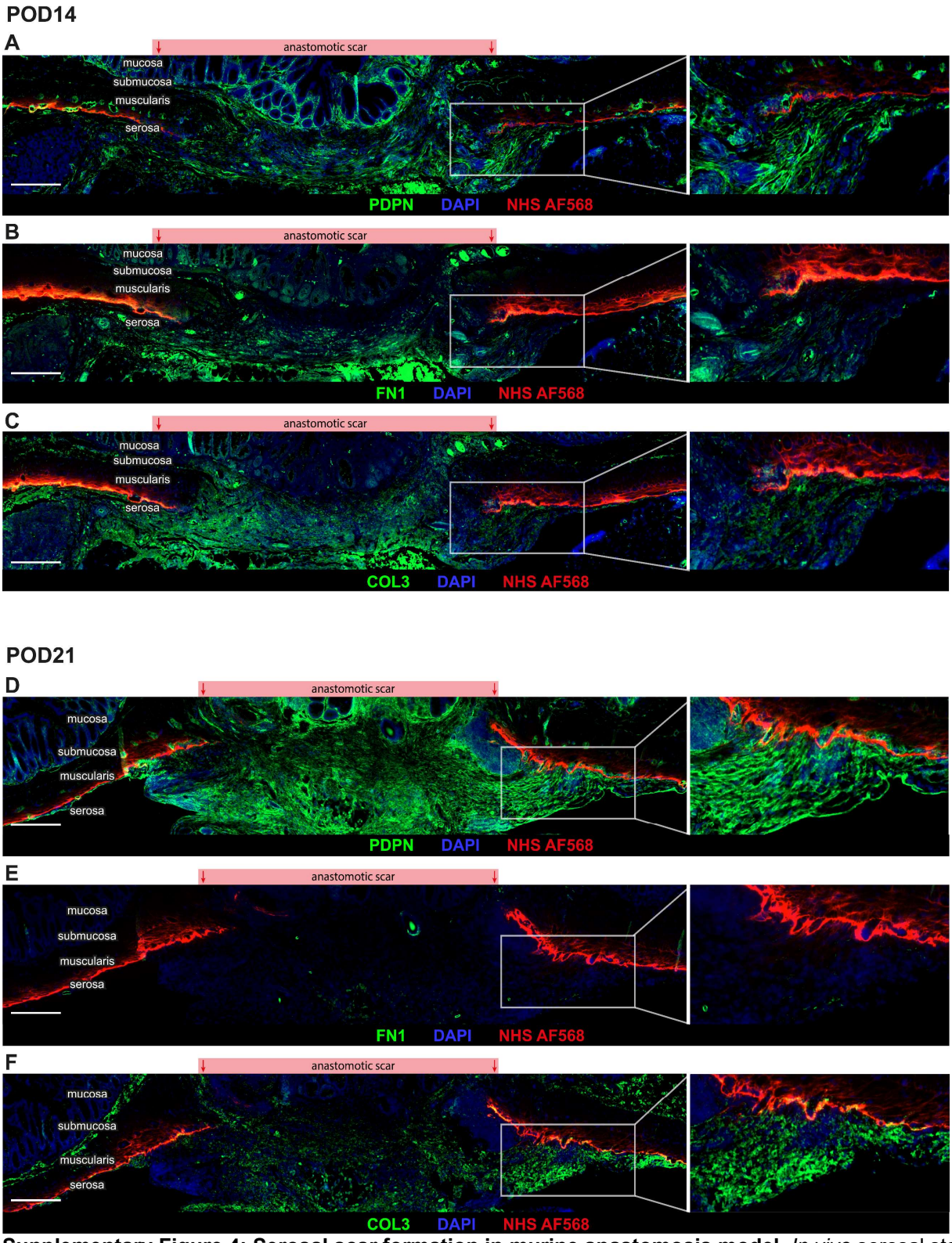

Supplementary Figure 4: Serosal scar formation in murine anastomosis model. *In vivo* serosal staining with NHS AF568 prior to anastomosis surgery and co-staining with **(A+D)** podoplanin (PDPN), **(B+E)** fibronectin (FN1) and **(C+F)** type III collagen (COL3). Representative images of anastomoses on postoperative days 14 (A-C) and 21 (D-F). Scale bar = 200µm, 100x magnification.

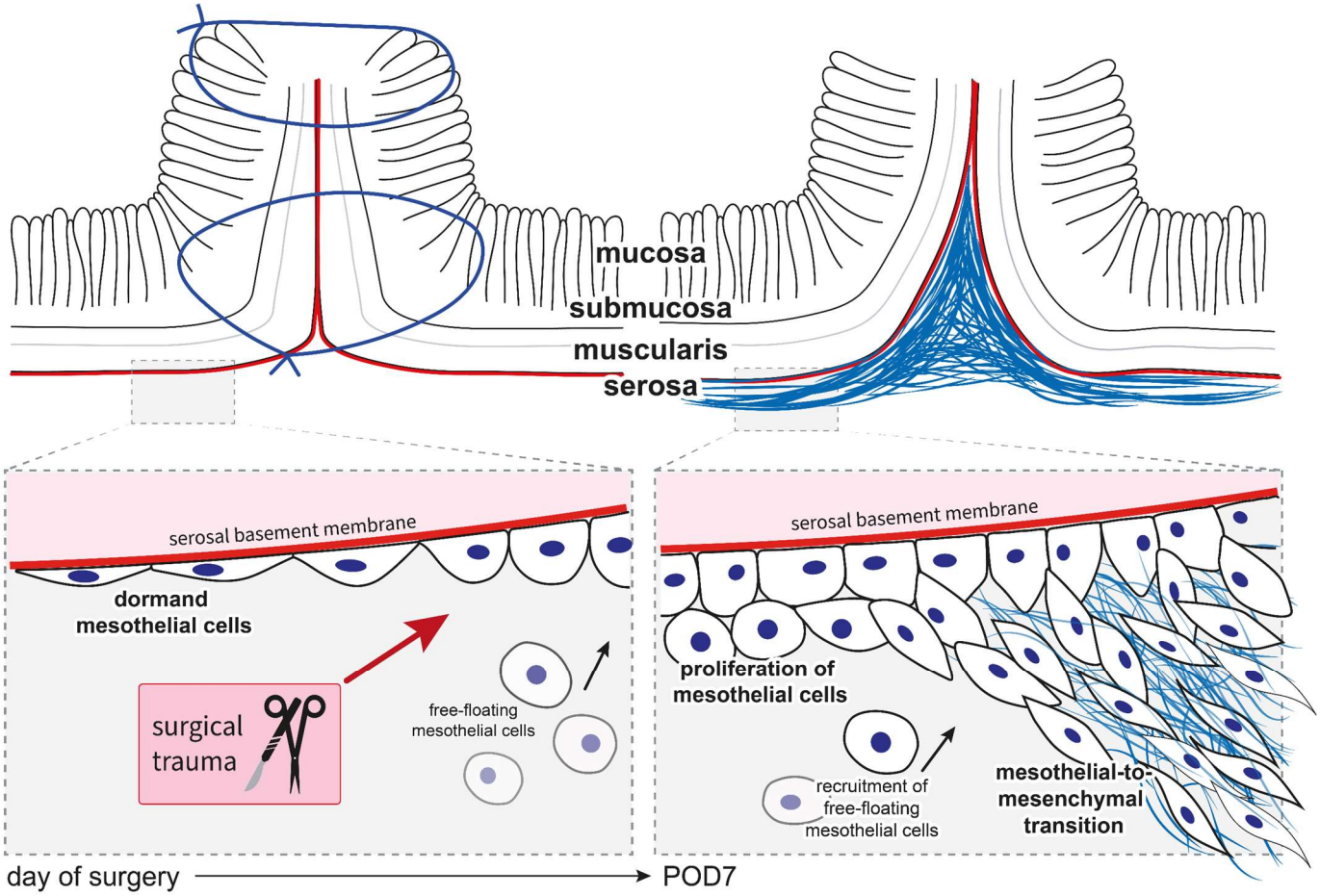

Supplementary Figure 5: Hypothetical model of mesothelial cell involvement in healing of intestinal anastomosis. We hypothesize that upon surgical trauma, local as well as free floating mesothelial cells proliferate and undergo mesothelial-to-mesenchymal transition (MMT) at the site of the anastomosis. Mesothelial cells thus initiate the production of extracellular matrix (ECM) for serosal scar formation during anastomotic healing in intestinal anastomoses.

4. Supplementary tables

Supplementary Table 2: *List of patient cases*

Case	Age of anastomosis	Type of anastomosis	Technique	Current surgery (anastomosis resection)		Previous surgery (anastomosis formation)		Patient age
				Type of surgery	Reason for surgery	Type of surgery	Reason for surgery	
1	7 days	jejunojejunal anastomosis	hand-sewn side-to-side double layered anastomosis	ileal resection including anastomosis	bleeding at anastomosis	ileum segment resection due	abdominal/peritoneal wall metastasis of colon cancer	73
2	9 days	ileocolonic anastomosis	hand-sewn side-to-side double layered anastomosis	oncologic right-sided hemicolectomy	incidental histologic cancer finding	ileocecal resection	acute small bowel obstruction at ileocecal valve with suspected Crohn's Disease	70
3	1,5 years	ileoileal anastomosis	hand-sewn side-to-side double layered anastomosis	ileocecal resection including anastomosis	Crohn's Disease: enterocutaneous fistula + stricturing ileitis terminalis	ileostomy closure	protective ileostomy due to colon perforation in the context of Crohn's Disease	52
4	2 years	colorectal anastomosis	end-to-end circular stapled anastomosis	tumor debulking with resection of transverse colon and colorectal anastomosis	ovarian cancer recurrence	tumor debulking including left sided hemicolectomy and lower anterior resection of the rectum	ovarian cancer	53
5	3 years	ileoileal anastomosis	hand-sewn side-to-side double layered anastomosis	ileal resection including anastomosis	small bowel obstruction distal of anastomosis	ileostomy closure	protective ileostomy for lower anterior resection of the rectum due to rectal cancer	80
6	7 years	ileoileal anastomosis	data not available	ileocecal resection including anastomosis	Crohn's Disease: stricture at ileocecal valve	ileum segment resection	stricturing Crohn's Disease	52
7	16 years	ileocolonic anastomosis	data not available	Right-sided hemicolectomy	Crohn's Disease: stricture colon ascendense/transversum	ileocecal resection	stricturing Crohn's Disease	57

6. References

1. Miltschitzky JRE, Clees Z, Weber MC, et al. Intestinal anastomotic healing models during experimental colitis. International journal of colorectal disease. 2021;36(10):2247-59.